Essential Readings in Light Metals: Cast Shop for Aluminum Production.
Edited by John F. Grandfield and Dmitry G. Eskin.

Light Metals — From *Light Metals 1986*, R.E. Miller, Editor

DEEP BED FILTRATION THEORY COMPARED WITH EXPERIMENTS

T.A. Engh*, B. Rasch* and E. Bathen**

*The Department of Metallurgy
The Norwegian Institute of Technology
7034 Trondheim, Norway

**SINTEF, 7034 Trondheim, Norway

INTRODUCTION

Filtration is an important unit operation in gas cleaning and in the purification of molten metals.

From a fluid mechanical point of view removal of particles from a gas and from a melt are very similar. Therefore it is here attempted to present a theory valid for both gases and liquids (melts). "Cake-filtration" is not dealt with. In the presentation we start out by studying removal to a single sphere, this theory is then stretched to include a packed bed of spherical particles based on published experimental correlations. Finally it is indicated how the correlation can be applied to beds containing non-spherical particles - for instance ceramic open pore filters.

The theory is compared with some published experimental results concerning removal of particles from gases and melts. Also a comparison is made with metallographic studies of removal of inclusions to graphite sampling filters and Selee open pore ceramic filters.

THEORY

Collection efficiencies for single spheres.

The collection efficiency η, of a spherical particle to a single sphere (in an infinite fluid) can depend on the following variables: diameter of collector d_c, diameter of particle d_p, velocity of fluid relative to collector u_∞ (far away from the collector), velocity of particle relative to liquid u_p (for instance due to gravity or buoyancy effects), the diffusion coefficient of the particles D, the densities of particle and fluid ρ_p and ρ_f respectively, and kinematic viscosity ν. Employing Buckinghams Π-theorem (1) it is found that the eight variables and three fundamental units m, s and kg give us 8-3 = 5 independent dimensionless groups. We may for instance choose:

$$Re_c = u_\infty \cdot d_c/\nu,\quad N = d_p/d_c,\quad Sc = \nu/D$$

$$\psi = N^2 \cdot Re_c \cdot (\rho_p + \rho_f/2)/18\,\rho_f \text{ and}$$

$$Re_p = u_p \cdot d_p/\nu$$

Here Re_c gives the Reynolds number referred to the approach velocity u_∞ and collector diameter d_c. For $Re_c < 1$ we are in the viscous flow region (2), while for $Re_c > 1$ a boundary layer is formed around the collector. N is a geometric group relating the size of the particle and collector. It plays an important role in describing the mechanism of removal by interception. Usually $N << 1$. This is the case especially in the removal of inclusions in melts where d_p is often in the range 0.1 to 10 µm while d_c usually lies between 100 to 1000 µm.

The Schmidt number determines the thickness of the diffusion boundary layer δ, relative to the convective boundary layer thickness δ_o (3):

$$\frac{\delta}{\delta_o} = Sc^{-1/3} \qquad (1)$$

For particle sizes between 0.1 and 10 µm, Sc is very large both for gases and fluids. For instance for air and molten aluminium $\nu \approx 0.01\ 10^{-3}$ m^2/s and $0.4\ 10^{-6}$ m^2/s respectively. For 1 µm particles the Stokes-Einstein equation

$$D = \frac{k_B \cdot T}{3\pi \cdot d_p \cdot \nu \cdot \rho_f} \qquad (2)$$

gives for air at room temperature and aluminium at 1000 K, respectively $3.6 \cdot 10^{-11}$ and $1.6 \cdot 10^{-12}$ m^2/s. Thus the Sc-numbers for air and aluminium become $Sc = 0.25 \cdot 10^6$ and $0.27 \cdot 10^6$. It is seen that the numerical values are not very different, around $3 \cdot 10^5$. This means that diffusion is controlled by the flow very close to the collector surface in both cases.

ψ called the inertial impaction parameter gives a ratio between inertial and viscous forces. In the literature a number of theoretical calculations and experimental results (4) are found relating η and ψ. In the calculations η is given as a function of ψ for various Re_c. Usually it is assumed that the particles have mass but no size, N = 0. For this inertial removal to be significant $\psi > 0.05$. In fluid filter systems this usually means that $Re_c >> 1$. In this case - assuming potential flow - the Langmuir-Blodgett calculations (5) may be employed.

For $\psi < 0.7$ we then have

$$\eta_{im} \approx (\sqrt{\psi} - 0.2)\cdot 0.4 \qquad (3)$$

It is seen that only when $\psi > 0.04$ do the particles cross the streamlines over to the collector surface.

Gravity η_g.

Re_p is the Reynolds number referred to the particles. Usually $Re_p << 1$ so that Stokes law may be employed to calculate the velocity of the particle relative to the surrounding fluid. Stokes law gives for the hydrodynamic force F acting on a sphere in an infinite fluid

$$F = 3\pi\, \mu \cdot u_p \cdot d_p \qquad (4)$$

Eq (4) is not valid near a wall or near other particles. The additional forces that then must be taken into account tend to displace the particle away from the walls (6). It is difficult to determine how important these forces are. Here it is only assumed that eq (4) is valid. Equating eq (4) to gravity minus buoyancy forces then gives:

$$u_p = \frac{(\rho_p - \rho_f)\, d_p^2 \cdot g}{18\, \rho_f\, \nu} \qquad (5)$$

where g is the acceleration of gravity, $g = 9.81\ m/s^2$.

For vertical flow through a filter one obtains

$$\eta_g = \frac{u_p}{u_\infty} \qquad (6)$$

Interception and diffusion, η_i, η_d.

In the literature (7-10) the η's for Brownian diffusion and interception are calculated for viscous flow, $Re_c < 1$ and for potential flow ($Re_c >> 1$). As pointed out previously, diffusion and interception effects are controlled by the flow very close to the collector - in the boundary layer for $Re_c > 1$. Therefore in this paper we first obtain relations for velocities in this boundary before calculating the η for the two mechanisms.

The stream function Ψ is given by (11):

$$\Psi = \sqrt{\frac{3\nu \cdot d_c \cdot U_\infty}{8}} \left\{ \theta\, f_1(v) - \theta^3\, f_3(v)/3 + \theta^5 \cdot f_5(v) \cdot 3/120 - - - - \right\} \qquad (7)$$

where the $f(v)$, $f_3(v)$ and $f_5(v)$ (11) are given as functions of

$$v = \frac{y}{d_c}\sqrt{6\, Re_c} \qquad (8)$$

y is the normal direction out from the spherical surface. θ is the angle between the fluid velocity and y. The tangential velocity is given by

$$u = \frac{\partial \Psi}{\partial y} \qquad (9)$$

Insertion of eq (7) in eq (9) results in:

$$u = \frac{3\, U_\infty}{2} \left\{ \theta \cdot f_1'(v) - \theta^3 \cdot f_3'(v)/3 + \theta^5 \cdot f_5'(v)\ 3/120 - - - - \right\} \qquad (10)$$

When $v \to \infty$ we have the potential flow velocity distribution. The boundary conditions for this case (11) are $f_1'(\infty) = 1$, $f_3'(\infty) = \frac{1}{2}$ and $f_5(\infty) = \frac{1}{3}$.

The collection efficiency for interception η_i may now be obtained from the relation

η_i = volume flow containing particles intercepting the sphere/volume flow approaching sphere (11)

The volume flow in the numerator is derived approximately as:

$$\int_0^y u \cdot 2\pi \cdot r \cdot dy = 2\pi\, \Psi \cdot r \qquad (12)$$

where r is the distance from the symmetry axis (see fig. 1).

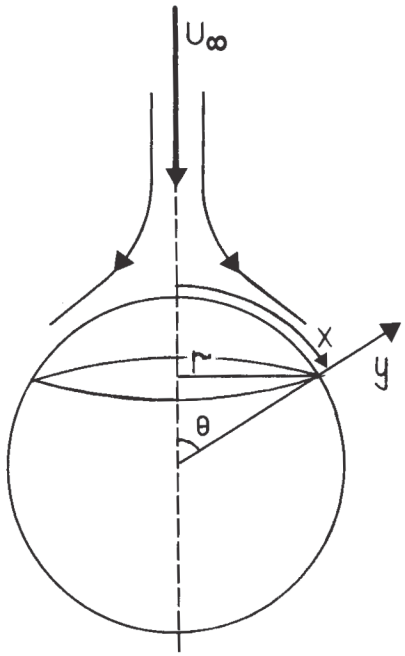

Figure 1. A spherical collector with some of the parameters used in the theory.

It is seen that

$$r = \sin\theta \, d_c/2 \qquad (13)$$

η_i obtains its greatest value for $\theta = \pi/2$. Equations (11-13) now give:

$$\eta_i = \frac{\pi \, \Psi(y = d_p/2) \cdot d_c}{\frac{\pi}{4} d_c^2 \cdot U_\infty}$$

or

$$\eta_i = \frac{4 \, \Psi \, (y = d_p/2)}{d_c \cdot U_\infty} \qquad (14)$$

For large particles giving $v > 1$ corresponding to the potential flow outside the boundary layer, $f_1(v) \approx v$, and the well-known formula is obtained

$$\eta_i = 3 \cdot N \qquad (15)$$

For small particles in the boundary layer $v < 1$ and $f_1(v) \approx 0.44 \, v^2$. Then eq (14) becomes

$$\eta_i = 0.4 \sqrt{Re_c} \cdot N^2 \qquad (16)$$

Eqs (15) and (16) apply only in the case that a boundary layer developes i.e. that $Re_c > 1$. For the case of creeping flow reference is made to the literature (7, 8). Removal by diffusion is treated theoretically in the literature for the case of creeping flow (2) and potential flow (12):

$$\eta_d = 4.1 \cdot (Re_c \cdot Sc)^{-2/3} \quad \text{for } Re_c < 1 \qquad (17)$$

$$\eta_d = \frac{8}{\sqrt{\pi}} (Re_c \cdot Sc)^{-1/2} \quad \text{for } Re_c >> 1 \qquad (18)$$

For intermediate Reynolds numbers, when $1 < Re_c$ and $v < 1$ the theory outlined here is employed. The method is similar to that used by Levich (2) for creeping flow. Then the diffusion equation

$$u \frac{\partial c}{\partial x} + u_n \frac{\partial c}{\partial y} = \frac{\partial}{\partial y} (D \, dc/dy) \qquad (19)$$

where u_n is the velocity in the y-direction, is transformed to an equation employing $x = \theta \, d_c/2$ and $p = \Psi \, r$ as independent variables.

$$u_n = - \frac{\partial(\Psi r)}{r \, \partial x} \qquad (20)$$

Eq (9) inserted in eq (19) then gives

$$\frac{\partial c}{\partial x} = D \, r^2 \frac{\partial}{\partial p} (u \frac{\partial c}{\partial p}) \qquad (21)$$

To solve this equation u must be found as a function of p. To accomplish this u and p are given as the following approximate equations (compare eqs (7) and (10):

$$p = \sqrt{\frac{3\nu \, d_c \, U_\infty}{8}} \cdot \frac{d_c}{2} \sin^2\theta \, f_1(v) \qquad (22)$$

where $f_1(v) \approx 0.44 \, v^2$.

$$u = \frac{3 \, U_\infty \cdot \sin\theta \, f_1'(v)}{2} \qquad (23)$$

where $f_1'(v) = 0.88 \, v$. We now eliminate v employing eqs (22) and (23):

$$u = 3.6 \cdot u_\infty \cdot Re_c^{-1/4} \sqrt{\frac{p}{\nu \cdot d_c}} \qquad (24)$$

Eq (24) inserted into eq (21) results in the following:

$$\frac{\partial c}{\partial t} = \frac{\partial}{\partial p} (\sqrt{p} \cdot \frac{\partial c}{\partial p}) \qquad (25)$$

where

$$t = \frac{0.45 \cdot D \cdot d_c^3 \cdot U_\infty \cdot Re_c^{-1/4}}{\sqrt{\nu \cdot d_c}} \int_0^\theta \sin^2\theta \, d\theta \qquad (26)$$

The solution of eq (25) integrating over angles from 0 to the "point of separation" of the flow at 109.6° gives for the number of particles reaching the sphere per unit time

$$I = 1.9 \, \nu^{1/3} \, D^{2/3} \, d_c \cdot Re_c^{1/2} \cdot c_o \qquad (27)$$

where c_o is the concentration [number/m^3] of particles far away from the collector.

The collection efficiency becomes

$$\eta_d = \frac{I}{\frac{\pi}{4} d_c^2 \, U_\infty \, c_o} = 2.4 \cdot Re_c^{-1/2} \cdot Sc^{-2/3} \qquad (28)$$

This result is the same as that obtained from the Frössling equation (13) and the well known Ranz-Marshall correlation (14) for mass transfer of a dissolved component in a gas or liquid.

Strictly speaking removal by diffusion should be calculated not at $y = 0$ but at $y = d_p/2$ corresponding to the position of the particles when they reach the surface. This approximation is acceptable in the part of diffusion boundary layer where concentration changes linearly with y. The thickness of the convection boundary layer is determined roughly by $v = 1$ or

$$\delta_o = d_c / \sqrt{6 \, Re_c} \qquad (29)$$

Employing eq (1), it is found that eq (28) applies for $\frac{d_p}{2} < \delta = \delta_c \, Sc^{-1/3}$ or $N < 2 \, Sc^{-1/3}/\sqrt{6 \, Re_c}$.

For

$$N > 2 \, Sc^{-1/3}/\sqrt{6 \, Re_c} \qquad (30)$$

we assume that resistance to particle transfer in the diffusion boundary layer becomes negligible. In this case transfer outside the diffusion boundary layer plays a role in particle transfer (12, 13, 14). Then the theories became very complicated, non-steady motion of fluid and particles must be taken into account, and experimental results are partly contradictory. Also surface roughness plays a role. However, the following line of reasoning seems to be fruitful: Since resistance in the diffusion boundary layer is unimportant, D and Sc no longer enter into the equations. Furthermore, usually Re_p will be small indicating that relative velocities between fluid and particles are small; the particles move together with the surrounding fluid. The ratio ρ_p/ρ_f does not affect the transfer. Finally, the surface roughness is due only to the particles already deposited. Of the 5 dimensionless groups this leaves only two Re_c and N.

Collection efficiencies for packed beds of spheres.

Experimental results for aerosols (7) indicate that in the case mentioned above, for $0.05 > N \, Re_c > 0.0075$ then

$$\eta \sim 0.5 \cdot N \cdot Re_c^{1/2} \qquad (31)$$

Eq (31) applies to a packed bed while previously only the collection efficiency for single spheres is presented. Often only the superficial velocity u_s is given in practical filter problems. Then u_∞ may be obtained from the relation

$$u_\infty = u_s/\varepsilon \qquad (32)$$

where ε is the porisity of the granular bed filter; usually ε is approximately 1/2. Data on mass transfer of a dissolved component in packed beds of spheres (14) indicate that eq (28) should be modified to

$$\eta_d = 5.8 \cdot Re_c^{-0.4} \, Sc^{-2/3} \qquad (33)$$

This is in rough agreement with (7).

Eq (18) is not valid for dissolved components due to the unrealistic assumption of potential flow in the diffusion boundary layer. However, for particles which are removed at a distance $d_p/2$ from the surface outside the diffusion boundary layer, eq (18) applies for $Re_c \gg 1$ and $N > 2\sqrt{6 \, Re_c} \, Sc^{1/3}$. No data is available concerning eq (18) employed for packed beds. It is assumed that the same correction factor applies to eq (18) as to eq (28). This gives

$$\eta_d = 11 \cdot Re_c^{-0.4} \, Sc^{-1/2} \qquad (34)$$

For interception the single sphere eqs (15) and (16) are used also for a packed bed of spheres. Interception may be regarded as removal by convection in the radial direction, at $y = d_p/2$ and should be added to removal by diffusion (at $y \gg d_p/2$). Removal by inertial impaction is also added even though it depletes c thus to some extent reducing the other η. Then the total collection efficiency η_t is given by:

$$\eta_t = \eta_i + \eta_d + \eta_g + \eta_{im} \qquad (35)$$

This gives for $Re_c \gg 1$ and $\frac{N}{2}\sqrt{6 \, Re_c} \cdot Sc^{1/3} < 1$:

$$\eta_t = 0.4\sqrt{Re_c} \cdot N^2 + 5.8 \cdot Re_c^{-0.4} \, Sc^{-2/3} + u_p/u_\infty + \eta_{im} \qquad (36)$$

and for $Re_c \gg 1$ and $\frac{N}{2}\sqrt{6 \, Re_c} \cdot Sc^{1/3} > 1$

$$\eta_t = 3 \, N + 11 \cdot Re_c^{-0.4} \, Sc^{-1/2} + u_p/u_\infty + \eta_{im} \qquad (37)$$

If in addition to $\frac{N}{2}\sqrt{6 \, Re_c} \, Sc^{1/3} > 1$ also $0.05 > N \, Re_c > 0.0075$ then

$$\eta_t = 3 \, N + 0.5 \cdot N \cdot Re_c^{1/2} + u_p/u_\infty + \eta_{im} \qquad (38)$$

Usually the impaction term η_{im} will only play a role for particle/gas systems due to the factor $(\rho_p + \rho_f/2)/\rho_f$.

If the total collection efficiency for a single sphere is η_t, it is shown in the following that the efficiency of collection for a bed of depth L is

$$1-E = \exp\left[-\frac{3 \cdot (1-\varepsilon) \cdot L \cdot \eta_t}{2 \cdot \varepsilon \cdot d_c}\right] \qquad (39)$$

where $E = \frac{\text{number of particles removed}}{\text{number of particles into filter}}$.

Collection efficiencies for non-spherical collectors:

For non-spherical collectors the situation becomes more complex. The collection efficiency may still be defined as

$$\eta = \frac{\text{effective cross sectional area for removal}}{\text{area of collector projected in direction of flow}} \qquad (40)$$

If the specific contact area (surface area/unit volume fluid) is a, the ratio between the projected surface area and the collector surface is b, then removal in a vertical slice of thickness dx is given by the differential mass balance

$$-\dot{q} \cdot dc = ab \cdot \eta_t \cdot dx \cdot \dot{q} \cdot c \qquad (41)$$

Here $\dot{q}$ is the volumetric flow of melt so that $-\dot{q}\,dc$ is the number of particles removed from the melt in the slice per unit time. $a\,b\,\eta_t\,dx$ is the fraction of the melt volume where particles are removed. The right-hand side gives the number of inclusions transferred to the collectors per unit time. Integration down the filter to depth x gives

$$\frac{c(x)}{c_o} = 1 - E = \exp\left[-a \cdot b \cdot \eta_t x\right] \qquad (42)$$

a and b are quantities determined by the geometry of the filter and can be measured for instance using metallographic methods. For spheres

$$b = 1/4$$

$$a = \frac{6\,(1-\varepsilon)}{\varepsilon \cdot d_c}$$

To obtain η_t it is necessary to give more general definitions of the dimensionless groups mentioned in the introduction. Assuming that the particles are spherical, Re_c is calculated employing eq (32) while Sc and Re_p are unchanged. For melts we assume that the effect of the impaction mechanism is negligible so that ψ does not enter into the calculations. This leaves the problem of defining N.

The interception mechanism as given by eq (14) may be written in the form

$$\eta_i = \frac{P \cdot u_c \cdot d_p/2}{A \cdot u_\infty} \qquad (43)$$

where P is the length along the periphery and A is the cross-section of the collector as seen in the direction of flow. u_c is the velocity along this periphery. For spheres and potential flow

$\frac{P}{A} = \frac{\pi\, d_c}{\pi \cdot d_c^2/4} = \frac{4}{d_c}$ and $u_c/u_\infty = \frac{3}{2}$ giving eq (15).

In a packed bed the flow cross-section will tend to be reduced around the periphery of a collector (see Fig.2). As a rough approximation we assume that $u_c/u_\infty = \frac{3}{2}$ also in this general case. Defining

$$d_c = 4\,A/P \qquad (44)$$

eq (15) may then be retained.

Applying a similar kind of reasoning, it is suggested that eq (44) be used throughout leaving the equations unchanged.

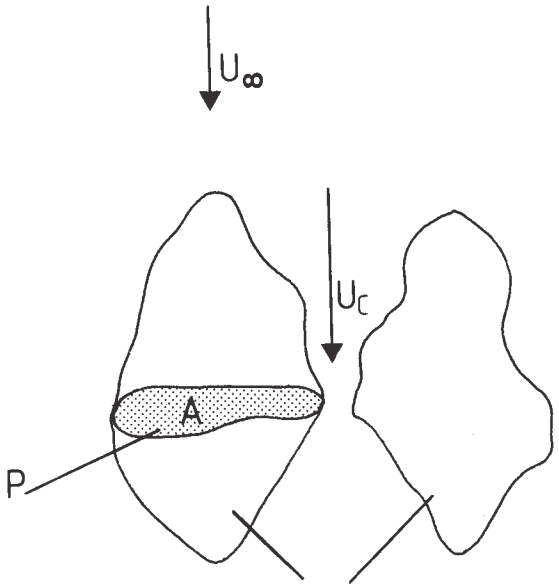

Figure 2. Non-spherical collectors. P is the length around the collector, A is the shaded area.

Figure 2 shows a collector and how cross-sectional area A and periphery length P is obtained.

Initial deposition in filter

The number of inclusions, N, collected in the filter after a time t at vertical position x per unit length of depth, N, is equal to

$$N(x) = \int_o^t \dot{q} \cdot a \cdot b \cdot \eta_t \cdot c \cdot dt \qquad (45)$$

Under steady-state conditions, and if the properties of the filter do not change with time:

$$N(x) \approx \dot{q} \cdot t \cdot a \cdot b \cdot \eta_t\, c(x) \qquad (46)$$

Deposition is proportional to concentration in the fluid at position x. This means that c(x) may be determined by counting the total number of inclusions deposited over time t at position x. Furthermore, $a \cdot b \cdot \eta_t$ can be calculated by combining eq (46) with eq (42). This gives

$$\frac{N(x)}{N(o)} = \exp\,(-\,ab \cdot \eta_t\, x) \qquad (47)$$

COMPARISON OF THEORY AND EXPERIMENTS, DISCUSSION

Published experiments

Mutharasan et coworkers (16) have performed filtration experiments using deep-bed filters. The filters consisted of either 2 cm alumina balls or 1-3 mm tabular alumina.

Table I shows measured filter efficiencies compared with out calculated values for the two types of deep-bed filters.

Table I. Measured filter efficiencies (by Mutharasan et co (16)) and calculated values

Type of filter	U_∞ (m/s)	$E_{meas.}$	$E_{calc.}$*	d_p (μm)
	$0.21\ 10^{-2}$	0.74	0.75	6
1-3 mm	$0.52\ 10^{-2}$	0.65	0.65	"
tabular	$0.75\ 10^{-2}$	0.52	0.62	"
alumina	$1.10\ 10^{-2}$	0.47	0.62	"
5 cm bed	$1.33\ 10^{-2}$	0.56	0.63	"
1-3 mm	$0.21\ 10^{-2}$	0.94	0.99	6
tabular al.	$1.25\ 10^{-2}$	0.73	0.99	"
25 cm bed				
2 cm alumina	$0.48\ 10^{-2}$	0.75	0.75	15
balls	$0.95\ 10^{-2}$	0.56	0.63	"
25 cm bed	$1.43\ 10^{-2}$	0.50	0.55	"

* using eq (38)

In the published experiments (16) the size of the TiB_2 particles were reported to lie in the range 1-30μm. The size distribution was not given. We found that a choice of inclusion diameter of d_p = 6 μm and d_c = 2 mm gave a good fit between calculated and experimental results for the tabular alumina. For the alumina balls it was necessary to choose d_p = 15 μm to give the correspondence shown in Table I.

The removal by the alumina balls seems to be surprisingly high compared to the tabular alumina. One explanation is the very high Re_c - up to 715; possibly eq (31) does not apply for such high Re_c giving $N\ Re_c = 0.05$.

Metallographic studies of filters.

Bathen (17) has developed a method for studying inclusions entrapped in filters by means of automatic image analysis. With this method inclusion size distributions and distributions by depth as well as the total amount of inclusions deposited in the filter can be determined. In addition to this the mean size of the grains (collectors) in the filter is measured using the mean intercept method.

Table II. Example of data from measurements on a graphite filter. The inclusions are Al_4C_3

Depth (μm)	Incl. in melt %	Melt of measured area (%)	No. of incl./mm² of melt in diff. size classes (μm) 1.45	2.2	2.9	3.6	4.3	5.1	5.8	Larger
0	12.2	59.8	14800	6560	1914	441	130	58	36	0
90	11.5	41.7	16300	6000	1704	343	118	11	11	0
130	8.9	38.7	14050	5380	808	480	212	33	11	11
330	6.4	42.9	8140	2715	827	388	82	31	10	10
500	2.6	46.1	4750	873	171	30	10	10	0	-
750	2.5	45.7	4220	680	283	57	9	0	30	10

Table II shows an example of some of the data that can be obtained employing this method.

Fig. 3 shows a plot of number of inclusions/mm² melt for the same filter. As can be seen from this figure the amount of particles decreases as we go down into the filter, but the size distribution does not change significantly.

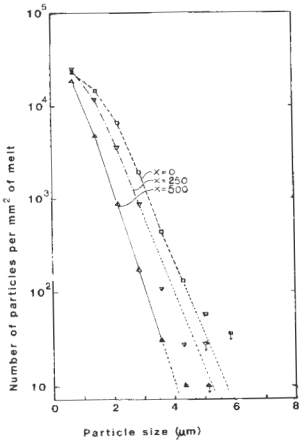

Figure 3. Number of particles/mm² melt in the filter as a function of particle size at three different depths.

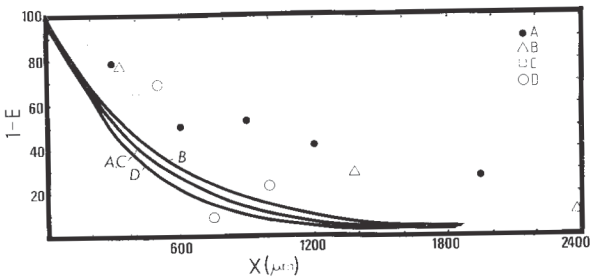

Figure 4. Measured and calculated particle concentrations for four different filters. The spherical model is used.

In fig. 4 measured and calculated particle concentrations are shown as a function of the depth in the filter. The calculated values are found employing the sphere model eqs (38) and (39). As can be seen from this figure the calculated values are smaller than the measured ones.

Introducing the nomospherical model (eq. 42) it is seen from fig. 5 that the fit between measured and calculated values is better. In fig. 5 the product a·b relative to the spherical model is set equal to 0.5. By setting measured values equal to the theoretical, the a·b value in eq. (42) for each filter is found. The value of a·b = 0.5 with a standard deviation of 0.19 is found by taking the average of the 4 filters.

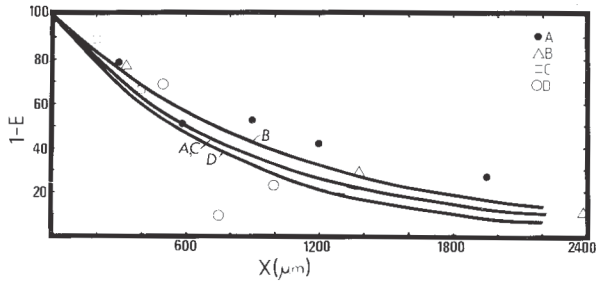

Figure 5. Measured and calculated particle concentrations for four different filters. Non-spherical model: (a·b) = 0.5.

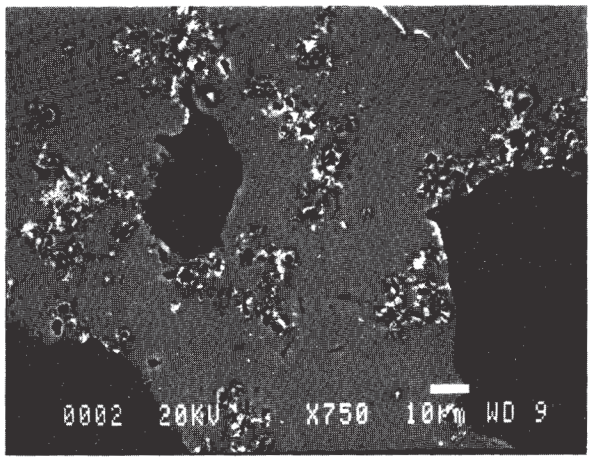

Figure 6. A Scanning Electron image showing agglomeration of particles. Big black areas are filter grains. Small black particles are carbides, white particles are TiB_2-particles.

CONCLUSION

Relations are given for the total efficiency of collection, η_t and for the overall efficiency of collection E - especially for spherical collectors. The theory seems to be sufficiently accurate to calculate the initial removal of inclusions in a filter from the collector diameter d_c, porosity ε, interstitial velocity u_∞ and inclusion diameter d_p. d_c may for instance be determined metallographically using the mean intercept method.

Ample experimental evidence exists (12-15) that at sufficiently large Reynolds numbers, Re_c, the collection efficiency increases with Re_c. This cannot be explained solely by the classical inertial impaction mechanism (eq. 3) where the particles must penetrate through the viscous boundary layer. Instead, the particles only have to impinge on roughness elements present initially or produced by deposition of some of the particles (see eq. 31). Eq (31) gives a rough estimate of this mechanism.

In the sampling filters the inclusions are found in "clusters" (see fig. 6). This may be explained by the mechanism mentioned above where particles tend to deposit close to "roughness elements" created by particles deposited previously.

According to table II the mean particle diameter is approximately 2 μm (on a volume basis) amd this value of d_p is used in the calculation in fig. 5.

The discrepancy between calculated and measured values in fig. 5 may be explained by difficulties in measuring a·b values for each filter and by the approximations involved in the theory.

In future work it will be attempted to determine a more accurate relation to replace 0.5 N $\sqrt{Re_c}$ in eq. (31). In addition to this a better and more accurate way of determining a·b values for the filters has to be found.

ACKNOWLEDGEMENT

The authors wish to acknowledge gratefully the financial rupport of the Royal Norwegian Council for Scientific and Industrial Research under project MB 61.15847 which made this research possible.

NOTATION

A	- projected area of collector perpendicular to the flow direction $[m^2]$
a	- specific contact area of the collector relative to a sphere
b	- ratio between projected surface area and collector surface area relative to a sphere
C, C_o	- particle concentration
D	- Brownian diff. constant $[m^2/s]$
d_c	- collector diameter $[m]$
d_p	- particle (inclusion) diameter $[m]$
E	- collection efficiency
I	- Defined by eq. (27)
k_B	- Bolzmann constant J/K
L	- filter depth $[m]$
N	$= d_p/d_c$
N(α)	- number of particles collected in the opening of the filter
N(x)	- number of particles collected at a distance x from the opening of the filter
P	- length along the periphery of a collector $[m]$
p	$= \Psi \cdot r$
$\dot{q}$	- volumetric flowrate of melt $[m^3/s]$
Re_c	- Reynolds number collector
Re_p	- Reynolds number particle

r - defined by eq (13)

Sc - Schmidt number (K)

T - temperature

U_c - melt velocity along the periphery of the collector [m/s]

U_p - particle velocity relative to melt [m/s]

U_s - superficial velocity [m/s]

U_∞ - U_s/ε [m/s]

v - defined by eq (8) [m]

x - depth in filter [μm]

y - distance from surface of collector [m]

δ - thickness of diffusion layer [m]

δ_o - thickness of convective boundary layer [m]

ε - porosity

η_d - diffusional collection efficiency

η_g - gravitational " "

η_i - interceptional " "

η_{im} - impactional " "

η_t - total collection efficiency

θ - given in fig. 1

ν - viscosity [m^2/s]

ρ_f - specific density of fluid [kg/m^3]

ρ_p - specific density of particles [kg/m^3]

Ψ - stream function

ψ - inertial impaction parameter

REFERENCES

1. J. Szekely, Fluid flow Phenomena in Metals Processing (Academic Press 1979), 409.
2. V. Levich, Physiochemical Hydrodynamics (Prentice-Hall, Inc. Englewood Cliffs, N.J., 1962), 80.
3. V. Levich, Physiochemical Hydrodynamics (Prentice-Hall, Inc. Englewood Cliffs. N.J., 1962), 59.
4. W. Strauss, Industrial Gas Cleaning, vol. 8, 2nd ed. (Pergamon Press), 280.
5. W. Strauss, Industrial Gas Cleaning, vol. 8, 2nd ed. (Pergamon Press), 284.
6. A. Ambari, B. Gauthier-Manuel, and E. Guyon, "Wall Effects on a Sphere translating at constant velocity," J. Fluid Mech., 149 (1984) 235-253.
7. N. Kimura et al., "Efficiency of Collection of Granular-Bed Filters due to Diffusion and direct Interception." Int. Chem. Engineering, 25,1, Oct. 1984, 122-129.
8. M. Beizaie, and C. Tien, "Particle Deposition on a single spherical Collector: A three-dimensional Trajectory Calculation," Can. J. Chem. Engineering, 58, Febr. 1980, 12-24.
9. C. Orr, ed., Filtration, Principles and Practices, Part 1 (Marcel Dekker Inc.) J. Pich, "Gas Filtration Theory".
10. H.J. Schulze, Physico-chemical elementary Processes in Flotation (Elsevier, 1984), 53-63.
11. H. Schlichting, Boundary-Layer Theory, 6th ed. (Mc Graw-Hill Book Corp., 1968), 223-228.
12. S.T. Johansen, "Particle Deposition on Surfaces from Turbulent Flows," (SINTEF report STF34A85-013, 1985) NTH 7034, Trondheim Norway
13. J.T. Davies, "A New Theory of the Deposition of Colloidal Particles from Turbulent Flows", Chem. Eng. Sci., 38 (1983) 135.
14. J.W. Cleaver, and B. Yates, "A Sub Layer Model for the Deposition of Particles from a Turbulent Flow," Chem. Eng. Sci. 30 (1975) 983-992.
15. Wakao and Kaguei, Heat and Mass Transfer in Packed Beds (New York N.Y., Gordon and Breach Science Publ, 1982), 156.
16. R. Mutharasan, D. Apelian, and C. Romanowski, "A Laboratory Investigation of Aluminium Filtration through Deep-bed and Ceramic Open-pore Filters", Journal of Metals Dec. (1981.
17. E. Bathen, "Investigation of Inclusions in Aluminium by Image Analysis", Proc. of the Int. Seminar on Refining and Alloying of Liquid Aluminium and Ferro-Alloys, Aug. 26-28 (1985) Trondheim, Norway. Aluminium-Verlag Düsseldorf.